Computation of Temperature Distribution in the Stator of a 75 kW Slip-Ring Induction Motor by FEM During Star-Delta Starting

Pradyumna Ranjan Ghosh* and Debasis Sarkar**
*Pradyumna Ranjan Ghosh, M.E. Student, EE Department, IIEST Shibpur,
prghosh2007@gmail.com
**Debasis Sarkar, Professor and Ex-HOD, EE Department, IIEST Shibpur,
debasissrkr@yahoo.co.in

Abstract: For development of electric machines, particularly induction machines, temperature limit is a key factor affecting the efficiency of the overall design, particularly during transient state. Since conventional loading of induction motors is often expensive, the estimation of temperature rise by tools of mathematical modeling becomes increasingly important and as a result of which computational methods are widely used for estimation of temperature rise in electrical machines. This paper describes the problem of two dimensional transient heat flow in the stator of induction motor during star delta starting. The stator being static is prone to high temperature and the study of thermal behavior in the stator is useful to identify the causes of failure in induction machines. The temperature distribution is obtained using finite element formulation and employing arch shaped elements in the r-θ plane of the cylindrical co-ordinate system. This model is applied to one 3-phase slip ring induction motor of 75 kW rating.

Keywords: Finite Element Method, Thermal Computation, Induction motor, Transient state Analysis, Design Performance.

Introduction

Traditionally, thermal studies of electrical machines have been carried out by analytical techniques or by thermal network method [8],[9]. Numerical techniques based on either finite difference method [10],[11] or finite element method [1]-[8] are more suitable for analysis of complex system. Most of the earlier designers and researchers have traditionally adopted analytical methods such as separation of variables, conformal mapping, and resistance analog networks for prediction of temperatures. The analytical work is largely limited and that too with many major assumptions. Even though the resistance analog method predicts average temperatures quite accurately, the method failed in predicting hot spot temperatures. Finite difference is one of the popular numerical methods widely used. The estimation of core iron and copper winding temperatures in electrical machines, the finite difference method had been normally employed. Even though this method predicts hot spot temperatures, the method is not as flexible as finite element method in handling complex boundary condition and geometry. Rajagopal [5] and Sarkar [7] have carried out extensive two-dimensional steady state and transient thermal analysis of TEFC machines using Finite Element Method (FEM). Recent advances in Computational Electromagnetics, encouraged by continuing increase of power and speed of computers, make finite elements and related techniques an attractive alternative to well established semi-analytical and empirical design methods, as well as to the still popular 'trial and error' approach.

In this paper, the finite element method is used for predicting the temperature distribution in the stator of an induction motor under transient state conditions, using arch-shaped finite elements with explicitly derived solution matrices. A general derivation of the finite element equations by the method of weighted residuals (Galerkin's method) is introduced. A 39-element two-dimensional slice of armature iron, together with copper winding bounded by planes at mid-slot, mid-tooth, are used for solution to a heating problem, and this defines the scope of this technique. The requirements of computer storage for a large number of elements have been reduced by the use of half band-width of the symmetric matrices so that the computing costs can be greatly reduced. The model is applied to one slip-ring induction motor of 75 kW rating and the temperatures obtained are found to be within the permissible limit in terms of overall temperature rise computed from the resulting loss density distribution.

Transient Heat Conduction

The general form of the heat conduction equation can be described by the following relations

$$V \nabla^2 T = P_m C_m \frac{\delta T}{\delta t} - Q \ \dots\dots\ (1)$$

where T is the potential function (temperature)

V is the medium permeability (thermal conductivity)

q is the flux (heat flux)

Q is the forcing function (heat source)

where P_m and C_m are material density and specific heat respectively

In cylindrical polar co-ordinates, equation (3) can be expanded as

$$\frac{1}{r}\frac{\delta}{\delta r}\left(V_r r \frac{\delta T}{\delta r}\right) + \frac{V_\theta}{r^2}\frac{\delta^2 T}{\delta \theta^2} + Q - P_m C_m \frac{\delta T}{\delta t} = 0 \ \dots\dots\ (2)$$

V_r, V_θ are thermal conductivities in the radial and circumferential directions respectively.

Finite Element Analysis (Galerkin's Method)

The Galerkin's criterion for heat conduction equations are used for furnishing thermal problems. When only the governing differential equations and their boundary conditions are available, Galerkin's methods are convenient in a way that this approach surfaces the variational method in generality and further broadens the range of applicability of the finite element method. Through the element equations derived for those problems were explicitly evaluated only for the simplest type in each case, the equations are general and apply for many element shapes and displacement models. The popularity of the method stems mainly from the case with which irregular geometries and implicit natural boundary conditions can be handled. Another important advantage is that the method allows development of general computer program that can solve variety of thermal problems simply by accepting different input data. The computer program illustrates how a real problem is actually solved by the finite element methods. It is envisaged that such programs would be useful for future studies of more complicated problems.

The solution of equation (4) can be obtained by assuming the general functional behavior of the dependent field variable in some way so as to approximately satisfy the given differential equation and boundary conditions. Substitution of this approximation into the original differential equation and boundary condition then results in some error called a residual. This residual is required to vanish in some average sense over the entire solution domain.

The approximate behavior of the potential function within each element is prescribed in terms of their nodal values and some weighting functions N_1, N_2 ... such that

$$T = \Sigma N_i T_i \ \dots\ (3)$$

i=1,2,….,m

The weighting functions are strictly functions of the geometry and are termed interpolation functions. These interpolation functions determine the order of the approximating polynomials for the heat conduction problem.

The method of weighted residuals determine the 'm' unknowns T_i in such a way that the error over the entire solution domain is small. This is accomplished by forming a weighted average of the error and specifying that this weighted average vanishes over the solution domain.

The required equations governing the behaviour of an element is given by the expression

$$\iint_{D^{(e)}} N_i \left[\frac{\delta}{\delta r}\left(V_r \frac{\delta T^{(e)}}{\delta r}\right) + \frac{\delta}{\delta \theta}\left(\frac{V_\theta}{r^2}\frac{\delta T^{(e)}}{\delta \theta}\right) + Q - P_m C_m \frac{2T^{(e)} - 2T_0^{(e)}}{2\Delta t}\right] r \, dr \, d\theta = 0 \dots (4)$$

where T_0 is the temperature at the previous point in time and Δt is the time interval

Equation (4) expresses the desired averaging to the error or residual within the element boundaries, but it does not admit the influence of the boundary. Since we have made no attempt to choose the N_i so as to satisfy the boundary conditions, we must use integration by parts to introduce the influence of the natural boundary conditions.

Arch Element Shape Functions

Consider the arch-shaped element of Fig. 1 formed by circle arcs radii a, b, radii inclined at an angle 2α.
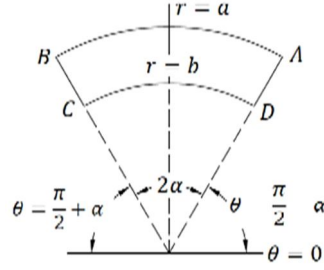
Fig. 1. 2D Arched shaped element suitable for discretization of induction motor stator

The shape functions can now be defined in terms of a set of non-dimensional coordinates with the help of cylindrical polar coordinates r, θ using the formula given below

$$\rho = \frac{r}{a}, \gamma = \frac{\theta - \pi/2}{\alpha}$$

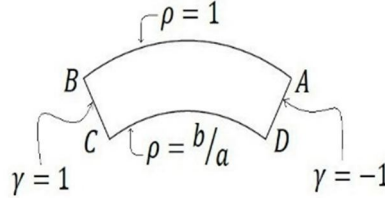The arch element with non-dimensional co-ordinates is shown in Fig. 2.

Fig. 2. The non-dimensional arch shaped element

The temperature at any point within the element be given in terms of its nodal temperatures by

$$T = T_A N_A + T_B N_B + T_C N_C + T_D N_D \dots (5)$$

Where the N's are shape functions chosen as follows:

$$N_A = \frac{(\rho - \frac{b}{a})(\gamma - 1)}{-2(1 - \frac{b}{a})} \quad N_B = \frac{(\rho - \frac{b}{a})(\gamma + 1)}{2(1 - \frac{b}{a})}$$

$$N_C = \frac{(\rho - 1)(\gamma + 1)}{-2(1 - \frac{b}{a})} \quad N_D = \frac{(\rho - 1)(\gamma - 1)}{2(1 - \frac{b}{a})}$$

Boundary Conditions

In this analysis the two dimensional domain of core iron and winding chosen for modelling the problem is shown in Fig. 3 and the geometry is bounded by planes passing through the mid-tooth and the mid-slot. The temperature distribution is assumed symmetrical across two planes, with the heat flux normal to the two surfaces being zero. From the other two boundary surfaces, heat is transferred by convection to the surrounding gas. It is convected to the air gap gas from the teeth, to the back of core gas from the yoke iron. The boundary conditions may be written in terms of $\frac{\delta T}{\delta n}$, the temperature gradient normal to the surface

1) Mid-slot surface $\frac{\delta T}{\delta n_s} = 0$

2) Mid-tooth surface $\frac{\delta T}{\delta n_t} = 0$

3) Air-gap surface $h(T - T_{AG}) = -V_r \frac{\delta T}{\delta n_{AG}}$

Where T=Surface temperature, T_{AG} =Air gap gas temperature

4) Back of core surface $h(T - T_{BC}) = -V_r \frac{\delta T}{\delta n_{BC}}$

Where T_{BC} = Back of core gas temperature

Approximate Numeric Form

The heat flow equation may be formulated in Galerkin's form, the solution being obtained by specializing the general functional form to a particular function, which then becomes the approximate solution sought. Focusing our attention on equation (4), we obtain through integration by parts.

$$\iint_{D^{(e)}} N_i \frac{\delta}{\delta r}\left(V_r \frac{\delta T^{(e)}}{\delta r}\right) r dr d\theta = \int_{S_2^{(e)}} V_r \frac{\delta T^{(e)}}{\delta r} n_r N_i d\Sigma - \iint_{r,\theta} V_r \frac{\delta T^{(e)}}{\delta r} \frac{\delta N_i}{\delta r} r dr d\theta \quad \dots (6)$$

Where n_r is the r component of the unit normal to the boundary, and $d\Sigma$ is a differential arc length along the boundary. Equation (6) takes the form

$$-\iint_{D^{(e)}}\left(V_r \frac{\delta T^{(e)}}{\delta r}\frac{\delta N_i}{\delta r} + \frac{V_\theta}{r^2}\frac{\delta T^{(e)}}{\delta \theta}\frac{\delta N_i}{\delta \theta}\right) r d\theta dr + \iint_{D^{(e)}}(N_i Q) r dr d\theta$$

$$-\iint_{D^{(e)}} \frac{P_m C_m}{2\Delta t}\left(2T^{(e)}N_i - 2T_0 N_i\right) r dr d\theta + \int_{S_2^{(e)}}\left(V_r \frac{\delta T^{(e)}}{\delta r} n_r + \frac{V_\theta}{r^2}\frac{\delta T^{(e)}}{\delta \theta} n_\theta\right) N_i d\Sigma^{(e)} = 0 \quad \dots (7)$$

For i=A, B, C, D

The surface integral (boundary residual) in equation (9) now enables us to introduce the natural boundary conditions. Equation (7) can be written with respect to the nodal temperatures as

$$\iint_{r,\theta}\left[V_r \frac{\delta T^{(e)}}{\delta r}\frac{\delta}{\delta T_i}\left(\frac{\delta T^{(e)}}{\delta r}\right) + \frac{V_\theta}{r^2}\frac{\delta T^{(e)}}{\delta \theta}\frac{\delta}{\delta T_i}\left(\frac{\delta T^{(e)}}{\delta \theta}\right) - QN_i\right] r dr d\theta$$

$$+\frac{P_m C_m}{2\Delta t}\iint_{r,\theta}\left[2[N]\{T\}^{(e)} N_i - 2T_0 N_i\right] r dr d\theta + \int_{S_2^{(e)}}\left(h[N]\{T\}^{(e)} N_i - hT_\infty N_i\right) d\Sigma^{(e)} = 0 \quad \dots (8)$$

For i=A, B, C, D

There are four such equations as (8) for the four vertices of the element. These equations, when evaluated lead to the matrix equation

$$\left[[S_R] + [S_\theta] + [S_T] + [S_H]\right][T] = [S_T][T_0] + [R] + [S_C] \quad \dots (9)$$

$[S_R]$, $[S_\theta]$ are symmetric coefficient matrices (thermal stiffness matrices)
$[S_H]$ is the heat convection matrix
$[S_T]$ is the heat capacity matrix
$[T]$ is the column vector of unknown temperatures
$[T_0]$ is the column vector of unknown (previous point in time) temperatures
$[R]$ is the forcing function (heat source vector)
$[S_C]$ is the column vector of heat convection

Method Of Solution [12]

The system of global equations as determined by equation (9) has to be solved in order to determine the nodal temperatures. The solution of this set of linear simultaneous equations is determined by Gauss method which takes the advantage of banded nature of the matrices. To save computer memory the symmetric matrix of half band width, efficiently stored by Gauss routine, by which extremely large problems can be effectively solved.

Application To Slip-Ring Induction Motor

The problem concerns heat flow through core iron and winding in the stator of an induction motor. The stator being static is prone to high temperature and the temperature distribution of the stator only is computed here. The hottest spot is generally in the copper coils. The heat from the outer surfaces, i.e. the back of core surface and the air-gap surface is lost through convective mode of heat transfer. Thermal conductivity of copper and insulation are taken together for calculation. As the temperature is maximum at the central plane, the temperature distribution in the plane can be determined approximately by taking this as a two-dimensional r-θ problem with the following assumptions:-

1) The temperature in the strip of unit thickness on the central axis is assumed to be fixed axially i.e., no axial flow of heat is assumed in the central plane. This assumption is permissible because in the central plane where the temperature distribution is maximum, the temperature gradient in the axial direction is zero.
2) The convection is taken care of only at the cylindrical surfaces neglecting the convection at the end surfaces.

Because of this assumption, the temperatures calculated in the central plane will be slightly higher than the actual.
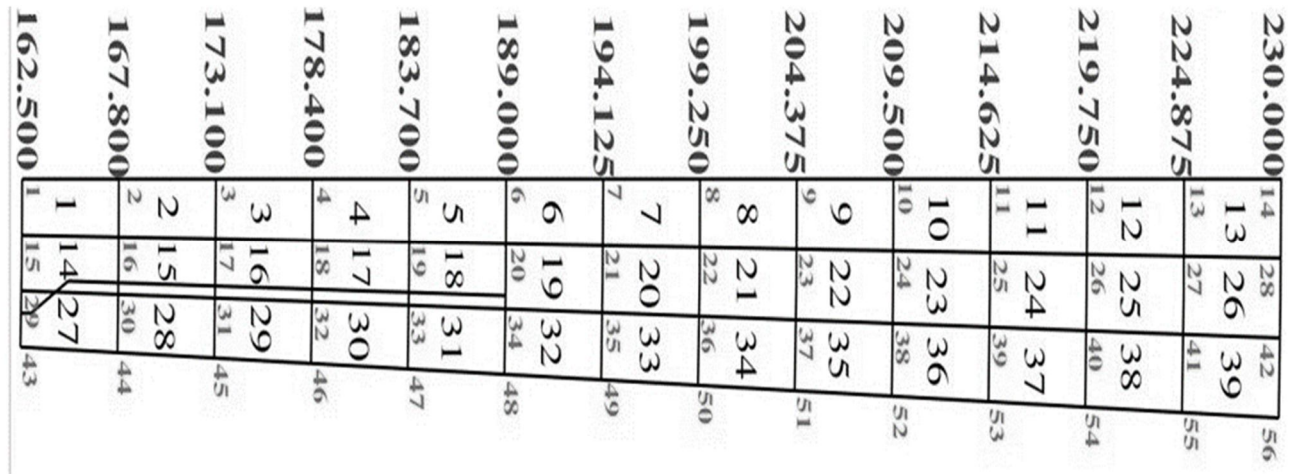

Fig. 3. Slice of core iron and winding of stator of slip ring induction motor bounded by planes at mid-slot and mid-tooth divided into arch shaped elements

In this analysis, because of symmetry the two dimensional domain in cylindrical polar co-ordinate of core iron and winding chosen for modeling the problem and the geometry bounded by planes passing through the mid-tooth and the mid-slot are divided into finite elements as shown in Fig. 3. Arch shaped elements are used throughout the solution region.

Convective Heat Transfer Coefficient
Two separate values of the convective heat transfer coefficient have been taken for the cylinder curved surface over the stator frame and the cylindrical air gap surface.
[1] Natural Convection:- The natural convection heat transfer coefficient on cylindrical curved surface over the stator frame are dependent on Grashof number and Prandtl number and calculated as h=4.795 watt/m^2 ^{0}C.
[2] Forced Convection:- The heat transfer co-efficient on forced convection for turbulent flow in cylindrical air gap surface are dependent on Reynolds number and Prandtl number and calculated as h= 76.84 Watt/m^2 ^{0}C.

Thermal Conductivity
For the steady state problem in two dimensions under considerations, the following properties are taken for each different material.
1) Thermal conductivity in radial direction, V_r Watt/m^{0}C
2) Thermal conductivity in circumferential direction, V_θ Watt/m^{0}C
3) Material density, P_m kg/m^3
4) Material specific heat, C_m watt sec/kg ^{0}C

Table 1. Typical Set Of Material Properties For Induction Motor Stator

Material Property	Magnetic Steel Wedge	Copper and Insulation
V_r	33.07	2.007
V_θ	0.826	1.062
P_m	7.86120	8.9684
C_m	523.589	385.361

Calculation Of Heat Losses [13]
Heat losses in the teeth and yoke of the core are based on calculated magnetic flux densities (1.56 wb/m^2 and 1.26 wb/m^2 respectively). In these regions, tooth flux lines are predominantly radial and yoke flux lines predominantly circumferential [13]. The grain orientation of the core punching's in these two directions therefore influences the heating for a given flux density. No significant change in flux density happens in stator core and tooth portions, thus their losses are kept constant as calculated during steady state operation [14]. Copper losses in the winding are determined from the length as well as the area

required for the conductors in the slot. The term star delta starting is applied to induction motors designed to run normally with delta connected stator winding. At starting, the stator winding is connected in star. After the motor has reached nearly to the steady state speed, i.e., 85% of the synchronous speed, the stator winding will be connected in delta.

Table 2. Heat Losses Generated At Different Time In Stator Slot Portion

	Slip s	Current (Amp) I	Stator copper loss /slot/unit volume (W/mm^3)	Δt (seconds)
Star Mode	1.0	762.107	0.0084393	
	0.8	750.080	0.008175	10.256946
	0.6	728.339	0.007708	8.325874
	0.4	680.828	0.006735178	6.4890195
	0.2	540.083	0.004238335	4.954262
Delta Mode	0.2	935.451	0.012715	
	0.1	611.928	0.005440952	0.7778345
	0.08	514.715	0.003849532	0.185265
	0.06	404.271	0.002374758	0.216777
	0.04	280.640	0.001144388	0.2799315
	0.0285	204.029	0.000604864	0.2207575
	0.02	144.760	0.000304488	0.2232975

Data Analysis

In this report the two-dimensional finite element method was applied to analyze the transient temperature rise in stator slice portion of 75 KW slip ring induction machine during star delta starting. The heat flux is assumed to be travelling along the stator of induction motor in order to obtain an optimum temperature distribution. It is observed that the stator copper loss has the highest value. So, it is evident that that the copper losses in the slot will have the highest operating temperature. Here class E insulation of copper winding is used whose maximum temperature is 120 $^{\circ}$C, so in no way the steady state temperature be greater than this value otherwise severe hazard will occur. Also it should not be operated at a much lesser temperature or else it would lead to under utilization of the machine. In the stator slice, node numbers 44 to 48 are present in the slot portion where the copper conductors are present and have maximum temperatures. It is observed that node number 47(slot portion) has the highest operating temperature of 115.419 $^{\circ}$C which satisfies the maximum permissible limit of temperature rise according to designer's specification. It is further observed that the value of temperature increases from air gap boundary surface towards the back of core surface. Temperature distribution profile in various parts of the machine of stator slot, tooth and core portions have been depicted in Figs 4, 5 & 6 respectively. From the result of transient temperature distribution in stator core and tooth, it is observed that the temperature of every node increases and then remains constant as we move along and across the surface of the core and tooth. Thus the stator core and tooth portion are not much affected during transient operation.
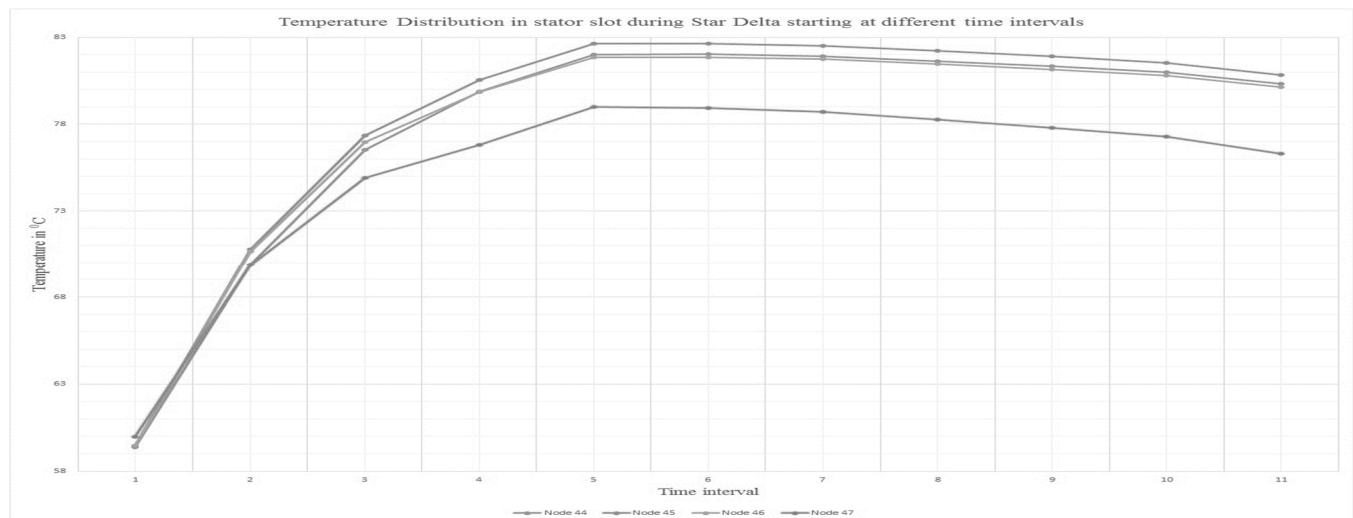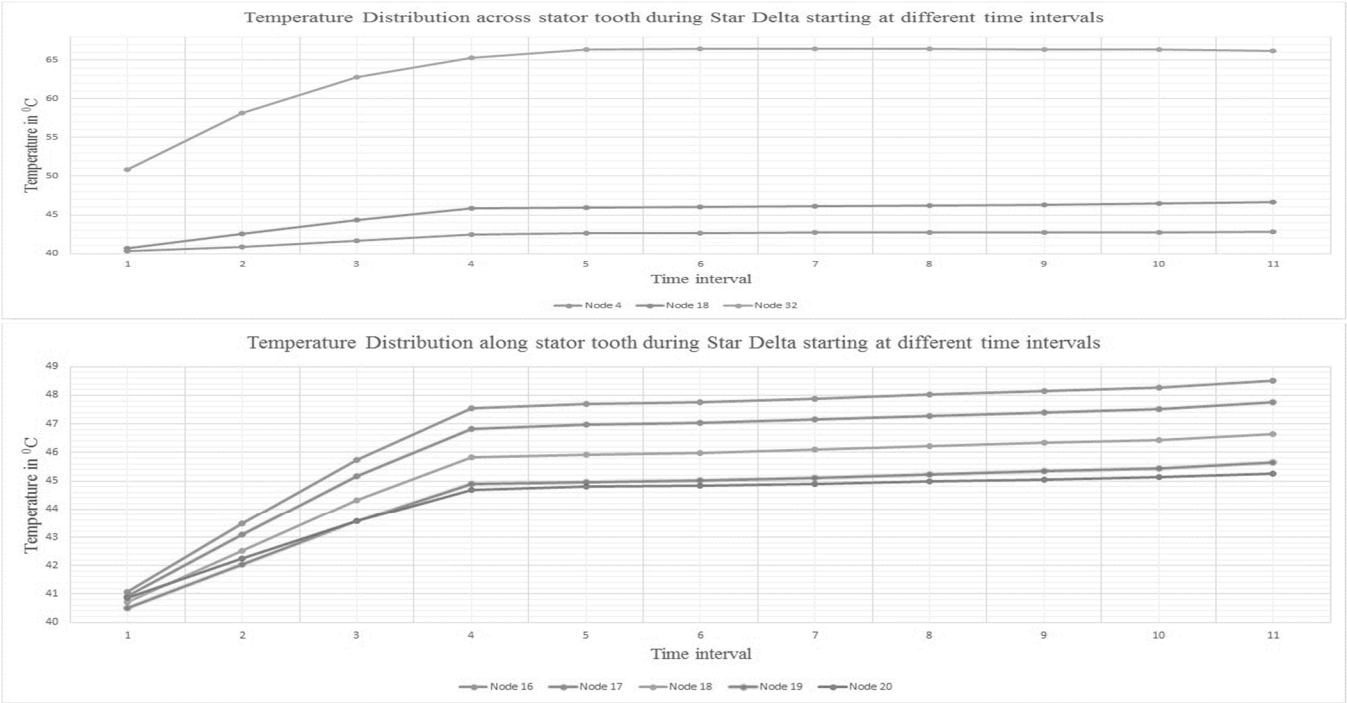

Fig 4:-Temperature Distribution in Stator Slot

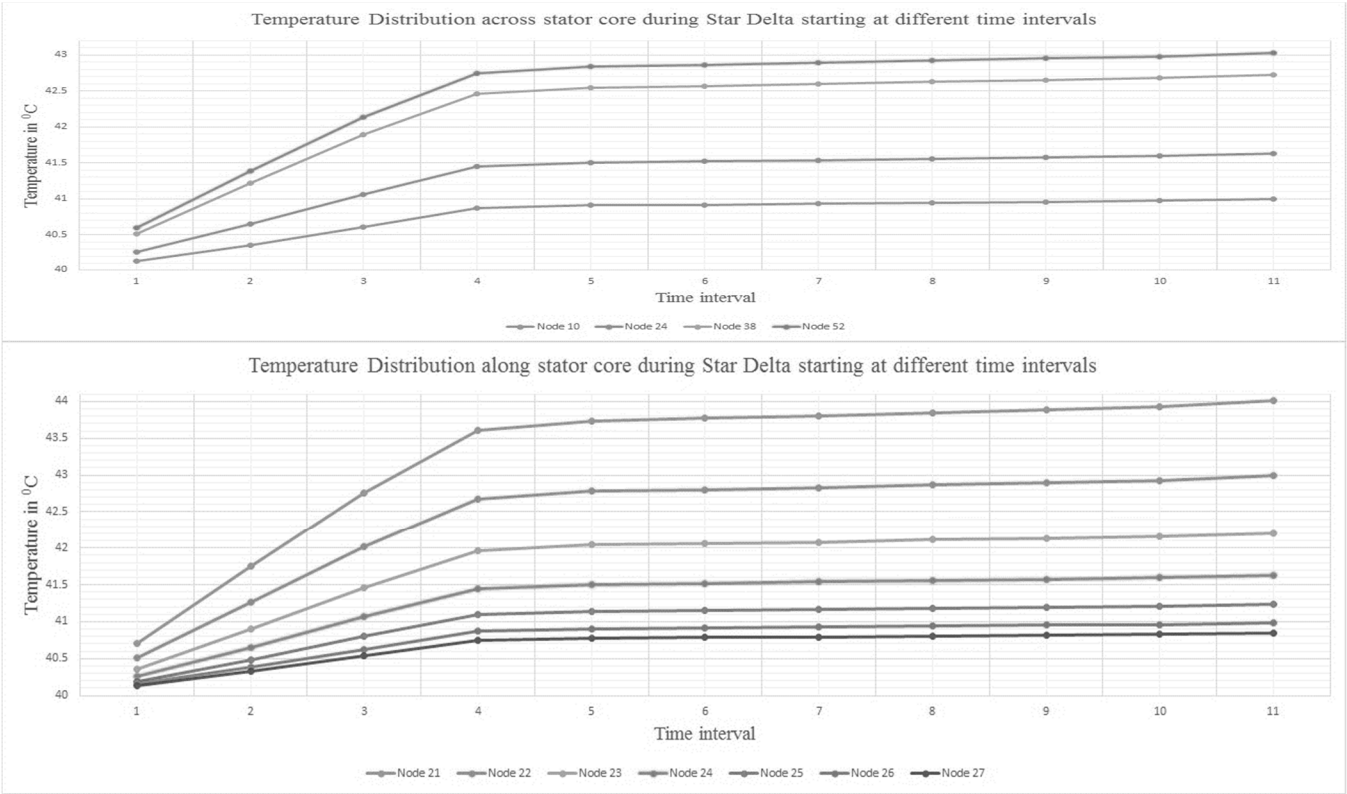Fig 5:-Temperature Distribution across and along Stator Tooth

Fig 6:-Temperature Distribution across and along Stator Core

Conclusion

The two-dimensional transient state finite element procedure for the thermal analysis of large induction motor stator provides the opportunity for the in-depth studies of stator heating problems. By virtue of the new, explicitly derived arch element, together with an efficient bandwidth and Gauss routine, extremely large problems can be efficiently solved. Though the results are approximate, the method is fast, inexpensive and leads itself to immediate visual pictures of the temperature pattern in a two-dimensional slice of iron core & winding in the stator of an induction motor. A number of other analysis can also be carried out, involving mechanical and electromagnetic fields, particularly where more than one of these fields are present.

References

[1] A.F.Armor., and M. V. K. Chari., "Heat flow in the stator core of large turbine generators by the method of three dimensional finite elements, Part-I:Analysis by Scalar potential formulation. Part - II: Temperature distribution in the stator iron," IEEE Trans,Vol. PAS-95, No. 5, pp.1648-1668, September 1976.

[2] A.F. Armor, "Transient, three-dimensional, finite element analysis of heat flow in turbine-generator rotors," *IEEE Trans. PAS-99*, no. 3, pp. 934–946, May/June 1980. .

[3] Boglietti, A. Cavagnino, D. Staton, Martin Shanel, M.Mueller, and C.Mejuto,"Evolution and modern approaches for thermal analysis of electrical machines", IEEE Transactions on Industrial Electronics", 56(3):871– 882, March 2009

[4] D. Staton, A. Boglietti, and A. Cavagnino., "Solving the more difficult aspects of electric motor thermal analysis in small and medium size industrial induction motors." Energy Conversion, IEEE Transactions on, 20(3):620–628, Sept 2005.

[5] M.S., Rajagopal,D.B.,Kulkarni,K.N., Seetharamu,and P.A. Ashwathnarayana., "Axi-symmetric steady state thermal analysis of totally enclosed fan cooled induction motors using FEM", *2nd Nat Conf.on CAD/CAM*,19-20 Aug,1994.

[6] W. Pepper and J.C. Heinrich. "The Finite Element Method: Basic Concepts and Applications. Series in Computational and Physical Processes in Mechanics and Thermal Sciences." Taylor & Francis, 2005.

[7] D. Sarkar, P. K. Mukherjee, and S. K. Sen, "Use of 3-dimensional finite elements for computation of temperature distribution in the stator of an induction motor," *IEE Proceedings*, pt. B, vol. 138, no. 2, pp. 75–86,1991.

[8] G. M. Rosenberry, Jr., "The transient stalled temperature rise of cast aluminium squirrel-cage rotors for induction motors," *AIEE Trans.*, vol. PAS-74, Oct. 1955.

[9] T. J. Roberts, "The solution of the heat flow equations in large electrical machines," *Proc. Instn. Mech. Engrs.*, pt.3E, vol.184, pp. 70–83, 1969–1970.

[10] K.Reichert,"The calculation of the temperature distribution in electrical machines with the aid of the finite difference method," Elektro Tech Z-A, Bd 90, H6, 1969.

[11] C. E. Tindall and S. Brankin, "Loss-at-source thermal modelling in salient pole alternators using 3-dimensional finite difference techniques," *IEEE Trans. Magnetics*, vol. 24, no. 1, Jan. 1988.

[12] L.L.,Bhirud,"Matrix operations on the computer", Bombay, Oxford & IBH Publishing Co., 1975.

[13] M.V.Deshpande, "Design and Testing of Electrical Machines", Wheeler Publishing, 1983

[14] Pradyumna Ranjan Ghosh, Nirmal Kr. Bhattacharya and Debasis Sarkar, "Computation of Steady State Temperature Distribution in the Stator of a 75 kW Slip-Ring Induction Motor by Finite Element Method", Fifth International Conference on Control System and Power Electronics – CSPE 2016

Appendix

A. Symmetric Coefficient Matrices

$$[S_R] = \frac{V_r \alpha}{6q^2}\left(1 - \frac{b^2}{a^2}\right)\begin{bmatrix} 2 & 1 & -1 & -2 \\ & 2 & -2 & -1 \\ & & 2 & 1 \\ SYM & & & 2 \end{bmatrix} \qquad [S_\theta] = \frac{V_\theta}{4\alpha q^2}\begin{bmatrix} A & -A & B & -B \\ & A & -B & B \\ & & C & -C \\ SYM & & & C \end{bmatrix}$$

Where $A = 1 - 4\frac{b}{a} + 3\frac{b^2}{a^2} - 2\frac{b^2}{a^2}\log_e\frac{b}{a}$, $B = -1 + \frac{b^2}{a^2} - 2\frac{b}{a}\log_e\frac{b}{a}$, $C = -3 + 4\frac{b}{a} - \frac{b^2}{a^2} - 2\log_e\frac{b}{a}$

B. Forcing Function Vector

$$[R] = \frac{Qa^2\alpha}{6\left(1 - \frac{b}{a}\right)}\begin{bmatrix} G \\ G \\ H \\ H \end{bmatrix}$$

Where $G = 2 - 3\frac{b}{a} + \frac{b^3}{a^3}$, $H = 1 - 3\frac{b^2}{a^2} + 2\frac{b^3}{a^3}$

C. Formulation Of The Heat Convection Matrix On Cylindrical Curved Surface

$$[S_H] = h\,a\,\rho\,\alpha \begin{bmatrix} \frac{2}{3} & \frac{1}{3} & 0 & 0 \\ & \frac{2}{3} & 0 & 0 \\ & & 0 & 0 \\ SYM & & & 0 \end{bmatrix}$$

D. Formulation Of The Heat Convection Vector On Cylindrical Curved Surface

$$[S_C] = h\,T_\infty\,a\,\rho\,\alpha \begin{bmatrix} 1 \\ 1 \\ 0 \\ 0 \end{bmatrix}$$

E. Formulation Of The Heat Capacity Matrix On Cylindrical Curved Surface (Only For Transient Analysis)

$$[S_T] = \frac{P_m C_m a^2 \alpha}{36\, q^2 \Delta t} \begin{bmatrix} 2D & D & -E & -2E \\ & 2D & -2E & -E \\ & & 2F & F \\ SYM & & & F \end{bmatrix}$$

Where $D = 3 - 8\dfrac{b}{a} + 6\dfrac{b^2}{a^2} - \dfrac{b^4}{a^4}$, $E = -1 + 2\dfrac{b}{a} - 2\dfrac{b^2}{a^2} + \dfrac{b^4}{a^4}$, $F = 1 - 6\dfrac{b}{a} + 8\dfrac{b^2}{a^2} - 3\dfrac{b^4}{a^4}$